IOP Publishing Journal of Physics D: Applied Physics

J. Phys. D: Appl. Phys. **55** (2022) 013002 (18pp) https://doi.org/10.1088/1361-6463/ac27d2

Topical Review

Recent progress in 3D printing piezoelectric materials for biomedical applications

Yushun Zeng[1,2,6], Laiming Jiang[1,2,3,6], Qingqing He[4], Robert Wodnicki[1,2], Yang Yang[5], Yong Chen[3,4,*] and Qifa Zhou[1,2,*]

[1] Department of Biomedical Engineering, Viterbi School of Engineering, University of Southern California, Los Angeles, CA 90089, United States of America
[2] Roski Eye Institute, Keck School of Medicine, University of Southern California, Los Angeles, CA 90033, United States of America
[3] Daniel J. Epstein Department of Industrial and Systems Engineering, Viterbi School of Engineering, University of Southern California, Los Angeles, CA 90089, United States of America
[4] Department of Aerospace & Mechanical Engineering, Viterbi School of Engineering, University of Southern California, Los Angeles, CA 90089, United States of America
[5] Department of Mechanical Engineering, San Diego State University, San Diego, CA 92182, United States of America

E-mail: yongchen@usc.edu and qifazhou@usc.edu

Received 16 May 2021, revised 1 August 2021
Accepted for publication 17 September 2021
Published 6 October 2021

Abstract

Three-dimensional (3D) printing technology has attracted significant attention for fabricating piezoelectric materials due to its high efficiency and capability to produce complex structures. Motivated by the desire to address limitations in conventional methods for fabricating piezoelectric materials, this review first introduces commonly used 3D-printing technologies to fabricate piezoelectric materials. The advantages of the technologies are evaluated. Subsequently, typical piezoelectric materials produced by 3D-printing methods are specifically discussed. The properties of the printed materials, such as dielectric and piezoelectric properties, are presented. Significant applications of 3D-printed piezoelectric materials are further explored, highlighting the potential of fabricating 3D-printed piezoelectric materials for biomedical applications. Finally, future directions and opportunities for 3D-printed piezoelectric materials are highlighted.

Keywords: 3D printing, piezoelectric materials, biomedical devices

(Some figures may appear in colour only in the online journal)

[6] These authors contributed equally to this work.
[*] Authors to whom any correspondence should be addressed.

1. Introduction

With recent advances in biomedical devices, the requirements for materials and functionality that can meet the needs of such devices are increasing. Piezoelectric materials that can realize the mutual conversion of mechanical and electric energy have been widely applied in ultrasonic imaging, energy harvesting, and bone engineering owing to their outstanding piezoelectric, mechanical and acoustic properties [1–6]. For example, due to the rapid development of advanced electronic devices, many of the shortcomings of traditional materials are related to reduced life span, and the replacement of batteries will result in low efficiency. Therefore, piezoelectric materials are gradually becoming an important option for replacing traditional materials in various applications [3, 7–10]. Various material fabrication methods have been utilized to address the increased demand for piezoelectric materials. Conventional strategies include mold forming, casting, and dice-and-fill techniques [11–15]. These methods can produce materials with excellent piezoelectric, ferroelectric characteristics and high density. However, with the revolution and rapid development of electronic technology, applied devices consisting of functional piezoelectric materials require structural diversity and micro-scalar size [16]. Hence, previous fabrication methods have come up against limitations including long fabrication times, high cost, and inability to fabricate complex shapes or microstructures. For example, with the tape casting method, piezo-powders are combined with solvents using ball milling for 24 h. Then plasticizers and binders are added for another 24 h via milling to render the mixture homogeneous [11]. The format of fabricated piezoelectric materials is typically limited to simple bulk shapes [17, 18]. Efforts to obtain three-dimensional (3D) structures with complex geometry and produce high-efficiency materials are needed to overcome these challenges. In recent years, 3D printing technology has been introduced as a newly emerging technique to fabricate complex structures using piezoelectric materials for various applications.

Additive manufacturing (AM), also known as 3D printing technology, has attracted attention in a number of fields due to its high-efficiency, high-resolution, low-cost, efficient utilization of material, and capability of fabricating intricate 3D structures [19–23]. Digital models of complex structures are usually designed using computer-aided design (CAD) software tools such as Solidworks and 3DMax. The CAD model is then sliced into several two-dimensional (2D) cross-sectional images for printing the 3D object layer by layer [24, 25]. A single layer thickness can be set at 50 μm or 100 μm [26]. Additionally, 3D printing methods can produce materials with isotropic or anisotropic performance via controlled filler alignment [27, 28]. Modern 3D printing methods include fused deposition modeling (FDM), stereolithography apparatus (SLA), and material jetting [23, 29–32]. 3D printing techniques have been widely applied to fabricate piezoelectric materials. Printable piezoelectric materials can be separated into organic, inorganic and composite [33–37]. Previous work reported fabrication materials with complex structures and the engineering of specific performance parameters of the end product. 3D-Printed piezoelectric composites have also drawn much attention. Recently, a flexible silver-coated PNN-PZT grid-composite with grid architecture based on a PDMS matrix was fabricated via the direct ink writing method, which demonstrated improved piezoelectric and electromechanical coupling coefficient [38]. Due to their advantageous material properties, 3D-printed piezoelectric materials have a bright future in biomedical research and products, such as wearable devices and energy harvesting.

This review aims to summarize recent advances in 3D-printed piezoelectric materials and highlight promising new applications of 3D-printed devices for biomedical applications. As shown in figure 1, first, the process and mechanism of the 3D printing methods will be described. Afterwards, categories of printable piezoelectric materials will be introduced. Then biomedical applications of 3D-printed piezoelectric materials such as ultrasonic devices, wearable devices, and implantable bone devices with a range of functionality, will be discussed and reviewed. Finally, future directions and challenges will be discussed, and the outlook for future research will be highlighted.

2. 3D printing methods for piezoelectric materials

Several 3D printing technologies have been used to fabricate piezoelectric materials, including FDM (FDM/material extrusion), selective laser sintering (SLS/vat photopolymerization), and stereolithography (SLA/powder bed fusion). The piezoelectric structures printed by the above techniques can be used to obtain piezoelectric properties after high-temperature sintering [39–44]. The first part of this review aims to discuss the different processes related to the above 3D printing technologies used to make piezoelectric components. Table 1 lists fabrication processes, fabricated molds, piezoelectric coefficient, and applications for commonly utilized 3D printable materials. According to various forming methods and different printable materials, each 3D printing technology has its advantages and disadvantages, these are highlighted and gaps during the development process are identified.

2.1. FDM

The FDM process is the most widely used 3D printing technology (figure 2(a)). It is also called fused filament fabrication, an AM process that belongs to the category of material extrusion [41, 55–57]. In FDM, an object is constructed by selectively depositing molten material in a predetermined path layer by layer. The material used in FDM is a thermoplastic polymer and is in the form of filaments [58, 59]. The FDM machine consists of three structural components: the feed roller, the guide sleeve, and the nozzle. FDM is suitable for the biological manufacturing of piezoelectric crafts and porous materials. In processing, first, the hot-melt filamentous material mixed with piezoelectric powder passes through the feed roller and enters the guide sleeve under the control of the driving roller. The low friction property of the guide sleeve allows the filamentous material to accurately and continuously enter the nozzle

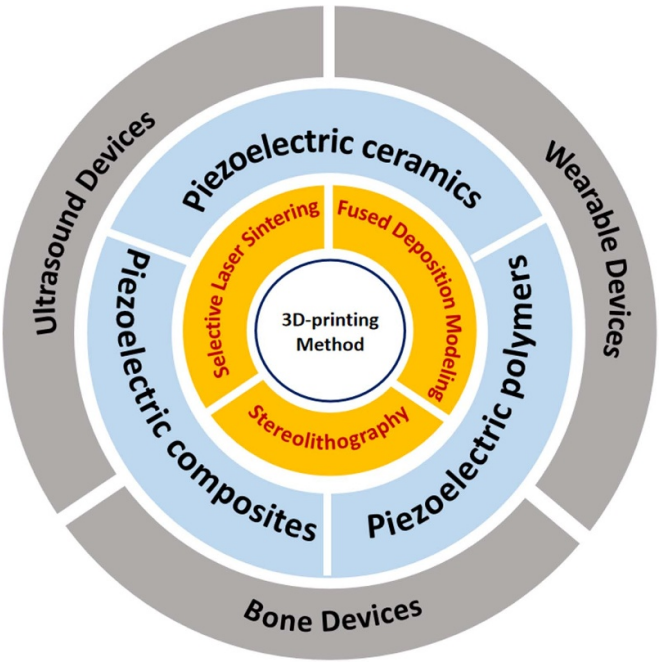

Figure 1. Integration of 3D printing for biomedical applications. The inset shows the categories of 3D printing methods, piezoelectric materials and their applications in biomedical areas.

[60, 61]. Polymers with piezoelectric powder are heated and melted in the nozzle, and then extruded out of the nozzle. A structure is 3D-printed according to the designed shape after the extruded piezoelectric polymer composite material is solidified due to the controlled low temperature [62–64].

Conventional production methods for volume manufacturing and prototyping of fine structures in fields such as medical devices and optoelectronics are routinely challenged when faced with more advanced complex structures. For example, to produce more complex ceramic tetrahedral structures, fused deposition of ceramics (FDC), an FDM technology, uses thermoplastic filaments to manufacture intricate structures. Bach *et al* applied FDC technology to manufacture grid structures (figure 2(b)) to obtain high-performance and functional piezoelectric ceramic structures [49]. High-load ceramic-EVA (vinyl ethyl acetate) was used as the raw material to combine with PZT powder. The research group successfully manufactured lead-free iron electric grid structures [49]. The PZT grid structure (figure 2(c)) was further processed into piezoelectric composite materials. The results of this research showed that maximal electromechanical properties can be achieved when the ceramic filling content is 70% by volume of ceramic [49]. Additional work in this area has been reported by Liu *et al*, who illustrated an ionic liquid (IL)-assisted FDM technology to directly print β-PVDF, where IL was able to induce and maintain β crystals in polyvinylidene fluoride (PVDF) polymer during melt extrusion [65]. Shear force from the FDM process resulted in self-polarization of the PVDF material. In a recent work illustrated in figure 2(d), a hemispherical protrusion array (HPA) was fabricated via the IL-FDM process, which showed improved piezoelectric output voltage and current density (17.5 nA cm^{-2}) [65]. In the future, one-step FDM printing methods like IL-FDM may be widely applied to obtain rapid fabrication of complex-structured piezoelectric devices. Although FDM can achieve a variety of material combinations and, therefore, different properties and material behaviors, there is still an opportunity to improve the accuracy and resolution of this printing process due to the limited selection of nozzle size dependent on minimum allowable filament diameter [66].

2.2. Stereolithography

SLA utilizes controlled light to cure a photopolymer and build up complex 3D structures in multiple 2D layers of photocured resin [67]. Depending on the type of light sources used, this 3D printing technique includes traditional laser-based stereolithography as well as digital light processing (DLP) based stereolithography (DLP-SL) [68, 69]. Laser-based SLA technology realizes the curing of a single layer by scanning of a laser spot [68, 69]. Through exposure of an ultraviolet (UV) laser beam, a layer section is solidified point by point, later from point to line, and then from line to surface [70]. 3D-printed piezoelectric parts are realized by superimposing multiple, individually photocured polymer layers while moving the printing platen in the *Z*-axis direction. In contrast, DLP technology cures single layers by projecting a mask image from a surface light source [71, 72]. Liquid resin that can be cured under UV light is used as a binder. When used for creating piezoelectric devices, the photocured resin is first mixed with piezoelectric powder to create a piezoelectric slurry [23]. A computer controls the UV light to irradiate the corresponding area according to the outline of each section, and the slurry quickly solidifies to form a 2D layer. By superimposing a succession of 2D layers directly on top of each other, newly solidified layers are bonded together to form a 3D object [23]. Light-cured forming technology is relatively mature and suitable for producing parts with complex structures and high precision requirements.

Figure 3(a) illustrates the projection-based SL process for a piezoelectric slurry, which induces curing using a light source. Ceramic stereolithography is related to an UV curable system which is made by the polymerization of ceramic particles suspended in a photopolymer. The technology has some limitations, including the fact that the refractive index difference between ceramic compounds and organic photosensitive structures causes reduction in printing efficiency, and the poor absorption rate of piezoelectric ceramic materials in the UV range leads to a reduced sensitivity to light cure in the slurry. The introduction of fine piezoelectric ceramic particles into the curable monomer results in a high level of complexity compared with traditional pure polymers. Light scattering by the fine piezoelectric ceramic particles will increase processing time and reduce curing depth and compromise the attainable *XY* resolution in the printing plane [73]. Hence, particle size and combined ratio of the piezoelectric powder are significant.

Combining with photocured resin, the volume or weight fraction of the piezoelectric powder in slurry plays an important role during the fabrication process. Hinczewski *et al* demonstrated that 53% volume fraction ceramic concentration

Table 1. Comparisons of 3D printable piezoelectric materials.

Printable materials	Fabricated process	Fabricated molds	Piezoelectric coefficient	Applications	Reference
PVDF	SLA and FDM	Polymers and composite	130 pC N^{-1}	Wearable devices	[45–47]
PZT	FDM and SLA	Ceramics and composite	345 pC N^{-1}	Ultrasound devices and wearable devices	[48–50]
KNN	SLA	Ceramics and composite	170 pC N^{-1}	Ultrasound devices	[51]
BTO	SLA and SLS	Ceramics and composite	160 pC N^{-1}	Ultrasound devices and wearable devices and bone devices	[20, 43, 52–54]

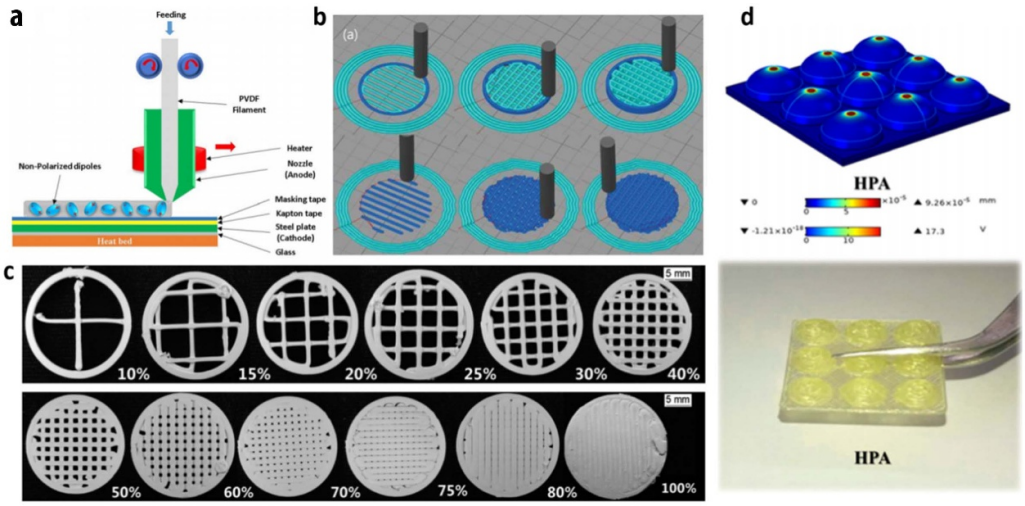

Figure 2. (a) Integrated FDM system. Reproduced from [57]. © IOP Publishing Ltd All rights reserved. (b) Schematic of FDC process for scaffold structure [49]; (c) printed PZT via FDC. Reprinted by permission from Springer Nature Customer Service Centre GmbH: [Springer Nature] [Springer eBook] [49], (2017). (d) A HPA model and optical image of HPA-PVDF device fabricated by IL-FDM. Reprinted with permission from [65]. Copyright (2021) American Chemical Society.

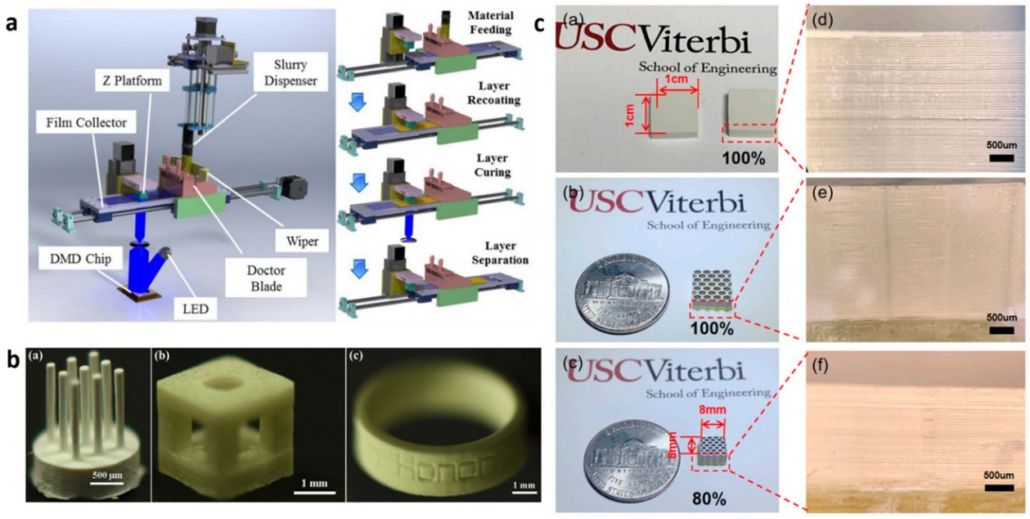

Figure 3. (a) A projection-based SLA process for piezoelectric slurry. Reproduced with permission from [23]. [Emerald Publishing Limited]. (b) Various SLA sample with complex structures printed by 40 vol% $BaTiO_3$ suspensions. Reprinted from [44], Copyright (2020), with permission from Elsevier. (c) Optical images of printed BTO honeycomb and brick structures. Reproduced from [20]. CC BY 4.0.

suspensions exhibit shear thinning behavior, which is beneficial for casting layers [74, 75]. To get high accuracy 3D ceramic particle printing, the size of particles must be smaller than the layer thickness in the fabrication process [74, 75]. In other work, Wang *et al* prepared high-performance piezoelectric nano-ceramics through stereolithography technology containing low-viscosity and high-solid content ceramic/polymer composite suspensions [44]. The maximum theoretical solid load, the rheological and solidification behavior of the suspension system were calculated from the experimental data. The material used in the experiment was a $BaTiO_3$ suspension, which is non-aqueous and has the characteristics of high solid content, low viscosity. The experimental data showed that the $BaTiO_3$ ceramic suspension with a high solid content of 40 vol% exhibits shear thinning behavior and low viscosity of 232 mPa s at a shear rate of 46.5 s^{-1}, which is advantageous for SLA. The analysis illustrates that the relative density of the $BaTiO_3$ ceramic components with nanometer-level grain size formed by the SLA printer is about 95% of the theoretical value. The components made have excellent dielectric properties ($\varepsilon_r = 2726$ and $\tan\delta = 0.016$ at 1 kHz) and the required piezoelectric constant ($d_{33} = 163$ pC N^{-1}). Moreover, several complex structures of the nine-rod array, hollow cube, and annulus were produced via the same SLA method with 40 vol% $BaTiO_3$ suspensions (figure 3(b)), demonstrating a novel strategy to fabricate functional 3D-geometry piezoelectric ceramic [44]. Additionally, a honeycomb composite structure and brick structure (figure 3(c)) were also fabricated via the mask image projection-based stereolithography (MIP-SL) method using a 70 wt% $BaTiO_3$ slurry. The sintered BTO honeycomb sample was poled under a DC electrical field of 20 kV cm^{-1} at room temperature for 30 min, demonstrating good piezoelectric coefficient ($d_{33} \sim 60$ pC N^{-1}) and ferroelectric properties ($P_{max} \sim 2.29$ μC cm^{-2}) [20]. These features can be applied to other devices to prove that SLA can be used to manufacture piezoelectric materials with intricate 3D shapes and acceptable piezoelectric properties.

2.3. SLS

SLS is a process that uses a powder bed as the material to be processed and an infrared laser to sinter this powder. The SLS process first uses a powder roller to spread a layer of the powder material, such as piezoelectric ceramic powder. The dispersed material is then heated to a temperature just below its sintering point using a constant temperature heating element that is integrated within the printing equipment. An infrared laser beam is focused on the powder layer to elevate its temperature above the melting point of the powder, thereby sintering and bonding the current layer with the previously sintered part below it [43, 76, 77]. After the existing single layer is sintered, the printing platen is lowered by the height of the layer thickness, and the powder spreading system spreads new powder material on the printing plates. The laser beam is again used for selectively irradiating active regions in the image for sintering, and so on, layer by layer, until the entire 3D-printed object is created [76–78]. Low precision, poor strength, and low density of SLS-printed piezoelectric parts have hindered the utility of SLS in production piezoelectric manufacturing. Additionally, due to the use of high-power infrared lasers, the technology is somewhat expensive and complicated to maintain. It is therefore not desirable for high-volume printing of piezoelectric components. These limitations for SLS fabrication of piezoelectric components can be mitigated to a certain extent by judicious selection of the materials and pretreatment processes which can improve somewhat the quality of samples fabricated using the SLS method.

Molding materials for the SLS process include a variety of powder materials with different mechanical properties and various nylon mixed materials. Some examples show mixtures of aluminum powder and nylon suitable for molds, mixtures of carbon fiber and nylon with extremely lightweight and strong mechanical properties, and a variety of mixed plastic materials and ceramic materials. In theory, any fusible powder can be used to make products or models, so the choice of powder material is one of the main advantages of SLS technology [79–84]. In previously reported work, nanocomposite powders for SLS were mixed in a solid-state shear milling reactor for pretreatment, which provides a strong shear force and improves the effects of pulverization, dispersion, and combination [85]. Qi *et al* also reported nanocomposite powders (polyamide11/$BaTiO_3$) that were prepared through a method combining solid state shear milling, melt blending and cryogenic grinding for use in SLS (figure 4(a)) [43]. The solid-state shear milling technique can enhance interfacial compatibilities and sintering windows (i.e. the temperature between the initial temperature of melting and crystallization). The resulting SLS-samples have improved dielectric constant (ε_r), piezoelectric coefficient (d_{33}), and piezoelectric voltage coefficient (g_{33}), as showed in figure 4(b) [43]. Ratsimba *et al* successfully manufactured objects with complex structures, including spheres and open loops using SLS [86]. Since the particle size and distribution of the powder bed affect development and packing density of the powder layer, the research team used optical techniques to measure the roughness of the powder bed, and established models through a dynamic discrete-element method (DEM) simulation based on experiments to estimate the density of the filled powder [86]. Moreover, Yang *et al* demonstrated a selective laser sintered poly-l-lactic acid scaffold with graphene and barium titanate (BTO), where graphene increased the electrical conductivity. In this case, BTO with excellent piezoelectric properties, was utilized as the ceramic filler. The electric field strength during poling was enhanced, which improved the overall piezoelectric response (output voltage of 1.4 V and current of 10 nA) [87].

3. 3D printing piezoelectric materials

The application of piezoelectric materials has brought about tremendous development in the field of biomedical engineering. The selection of suitable 3D-printable piezoelectric materials is the first step in AM. This choice largely depends on the specific device application, which directly

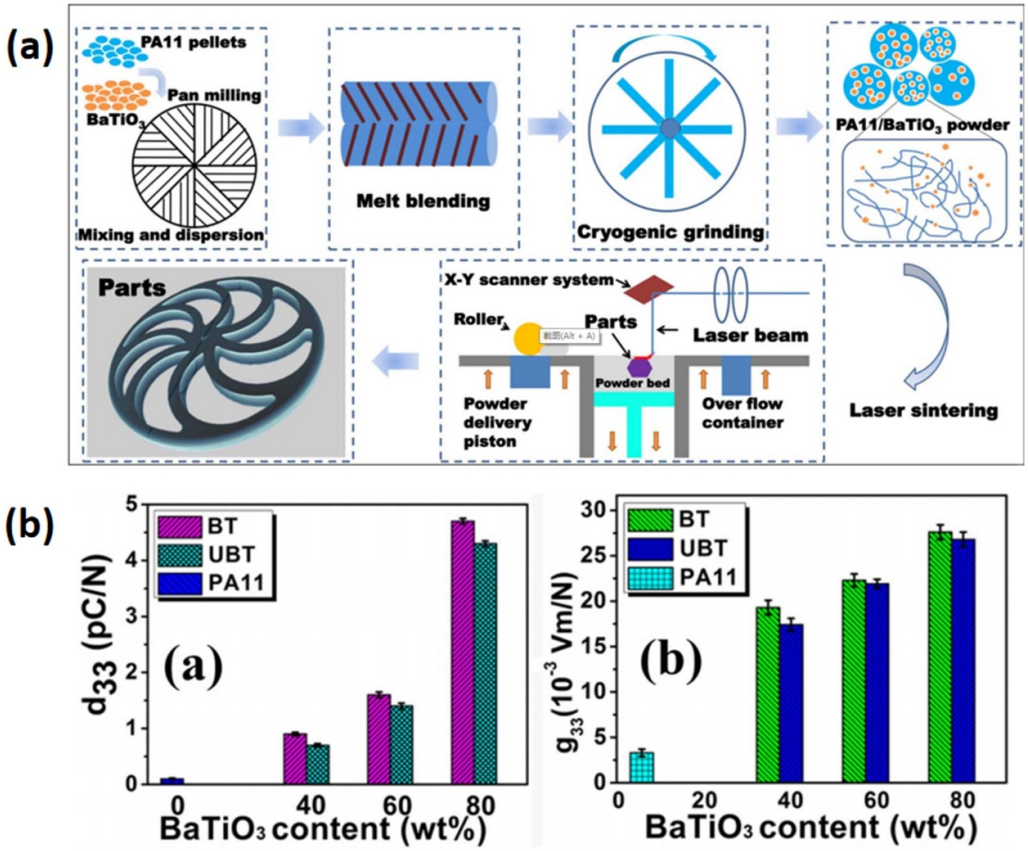

Figure 4. (a) Schematic of fabrication of PA11/BaTiO3 nanocomposite, and (b) piezoelectric performances of SLS-printed sample. Reprinted from [43], Copyright (2017), with permission from Elsevier.

affects its mechanical and electrical performance [16]. For instance, the piezoelectric coefficient and the acoustic properties of the 3D-printed piezoelectric material should be equivalent or better than that of piezoelectric material fabricated via traditional methods. For various biomedical applications, typical 3D-printed piezoelectric materials can be categorized as inorganic piezoelectric ceramics, organic piezoelectric polymers, and piezoelectric composite (organic/inorganic) materials [88–91]. They will be discussed in detail in this section.

3.1. Piezoelectric ceramics

With excellent mechanical, piezoelectric, and acoustic properties and being inexpensive to produce, piezoelectric ceramics have unique applications in biomedical engineering. The piezoelectric ceramic most commonly used in 3D printing is lead zirconate titanate (PZT) due to its excellent piezoelectric coefficient and ease of manufacturing [92]. In the previous work in this area, a PZT green part sample fabricated using SLA (figure 5(a)) was sintered, and demonstrated stable tetragonal phase. After poling in silicone oil at 70 °C under an electric field of 30–40 kV cm^{-1} for 15 min, the sintered sample achieved an optimized piezoelectric constant (212–345 pC N^{-1}) and dielectric constant (760–1390) [48]. The sintered PZT was also integrated to create a 2D array with a center frequency of 2.24 MHz for ultrasound transducer applications [48]. In general, poling piezoelectric materials at elevated temperature enhances the alignment of dipoles, which can strengthen the electromechanical coupling of the piezoelectric ceramics [93]. Hence both the efficiency of energy conversion and the fractional bandwidth (35%) of the device can be improved. The comparative low cost and ease of manufacture with these materials have made piezoelectric ceramics prevalent in industrial and medical applications. Recently, there has been significant research towards the possibility of using lead-free piezoelectric ceramics to replace lead-based materials due to increasing interest in materials that are eco-friendly and non-toxic to the human body [94, 95]. For this reason, 3D printing of lead-free piezoelectric ceramics for use in biomedical engineering has enjoyed increasing interest in recent years.

BTO was one of the first classic lead-free perovskite ceramic materials developed that exhibits excellent dielectric and piezoelectric properties. This material has been investigated and applied in AM for decades, due to its good performance, low cost, and accessibility [96, 97]. Recently, Zeng *et al* developed a MIP-SL based BTO ceramics fabrication process [20]. BTO powder was first combined with photocurable resin via ball milling to achieve homogeneous slurry for SLA to fabricate green parts (the 3D-printed objects before the sintering process). During debinding process, the temperature rises at a rate of 1 °C min^{-1} and will be held at 200 °C, 300 °C, 400 °C and 500 °C for 30 min, respectively. Afterwards, the

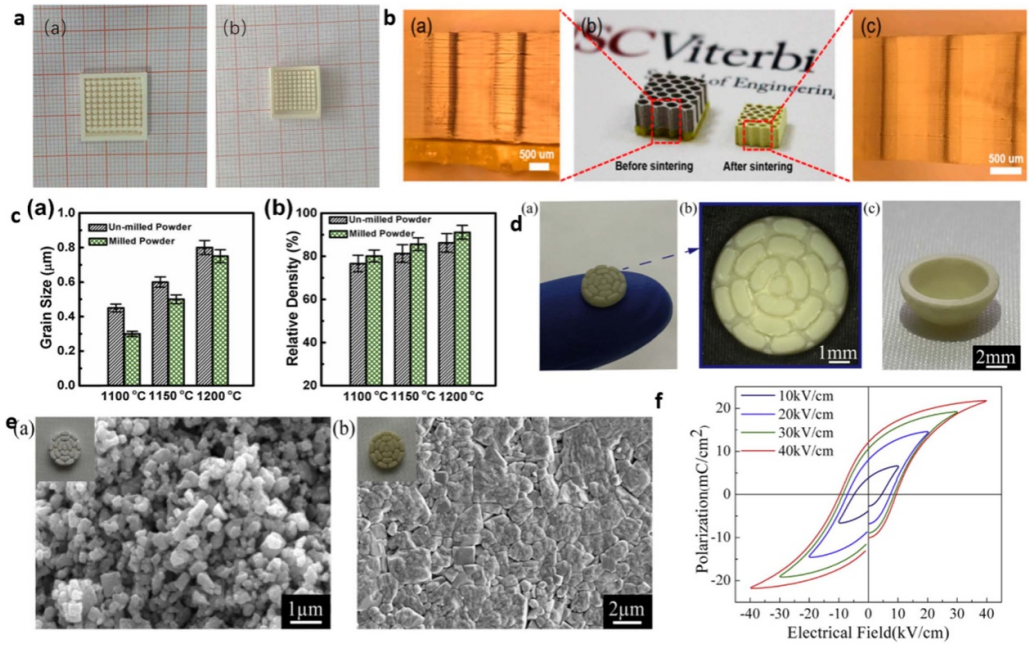

Figure 5. (a) Green part and sintered part of 3D-printed PZT array. Reprinted from [48], Copyright (2018), with permission from Elsevier. (b) SEM of 3D-printed BTO. Reproduced from [20]. CC BY 4.0. (c) Grain size and density of two types of BTO powders. Reprinted from [98], Copyright (2020), with permission from Elsevier. (d) Optical images of the sintered KNN piezoceramics [51], (e) SEM images of debinded and sintered KNN ceramic [51], and (f) polarization-electric field (*P–E*) hysteresis loop of the printed KNN ceramic under different electric fields. Reprinted from [51], Copyright (2019), with permission from Elsevier.

resin component of the green part was removed by heating at 600 °C for 3 h [23]. Sintering is vital to remove the resin inside the 3D-printed green part and make the sample denser (figure 5(b)), thus, debinded samples were placed in a regular furnace at 1340 °C for 4 h. After sintering, the structure of the 3D-printed BTO became denser, and the sintered sample demonstrated good piezoelectric and ferroelectric properties, with a piezoelectric constant of 60 pC N^{-1} and a maximum polarization of 2.29 μC cm^{-2} [20]. The weight ratio of the BTO was optimized up to 70% to realize successful printing [20]. Powder milling is a crucial process step to prepare fine particles for 3D printing. A comparison between milled and unmilled samples was investigated by producing BTO via extrusion free-forming derived from milled precursors [98]. In figure 5(c), the milled samples had a smaller grain size (0.8 μm) and higher relative density (90%) with increased annealing temperature. The improved density, in turn, leads to improved sinterability, yielding an optimized dielectric coefficient (d_{33}), which was enhanced from 290 to 360 pC N^{-1} after prolonged sintering [98].

Additional research by Chen *et al* demonstrated the use of micro-SLA to produce KNN-based lead-free piezoceramics to create a segmented annular array with a pitch of 1 mm on a hollow hemispherical structure (figure 5(d)). Figure 5(e) shows SEM images that highlight how the porous structure of the original green body ceramic was removed from the printed piezoelectric sample after sintering [51]. The measured piezoelectric constant was 170 pC N^{-1}. The ferroelectric properties of the fabricated material are illustrated in figure 5(f), which shows the measured polarization-electric field (P–E) hysteresis loop. These results successfully demonstrated an alternative method for the fabrication of KNN lead-free piezoceramic components with complex architectures for biomedical applications [51]. The benefits of 3D printing lie in time-savings, the convenience of fabricating piezoceramics with complex structures, and the ability to obtain piezoelectric properties comparable to traditional processes. For 3D-printed piezoceramics, the weight ratio of the mixed ceramic powder, combination of functionalization agent, sintering time and temperature gradient all need to be further optimized to improve relevant piezoelectric properties. In addition, further work in 3D printing of lead-free piezoelectric ceramics is required to select proper materials to achieve the goal of replacing leaded materials for device manufacturing. Therefore, the development of novel piezoelectric ceramics for 3D printing is currently an active area of research.

3.2. Piezoelectric polymer

The development of flexible electronics has required the use of materials that are flexible and can be twisted and stretched while preserving their original electrical and structural properties [99, 100]. In the past, brittleness and rigidity have limited traditional piezoceramics in applications requiring flexible devices. Therefore, flexible piezoelectric polymers with excellent piezoelectric properties have received increasing attention in various areas, especially in the biomedical field. PVDF and its copolymers are the most representative and commonly utilized piezoelectric functional polymers [101, 102]. PVDF is synthesized via polymerization of vinylidene difluoride, assuming crystal forms with α, β, γ, and δ phases [103, 104]. Significantly, β-PVDF has excellent ferroelectric

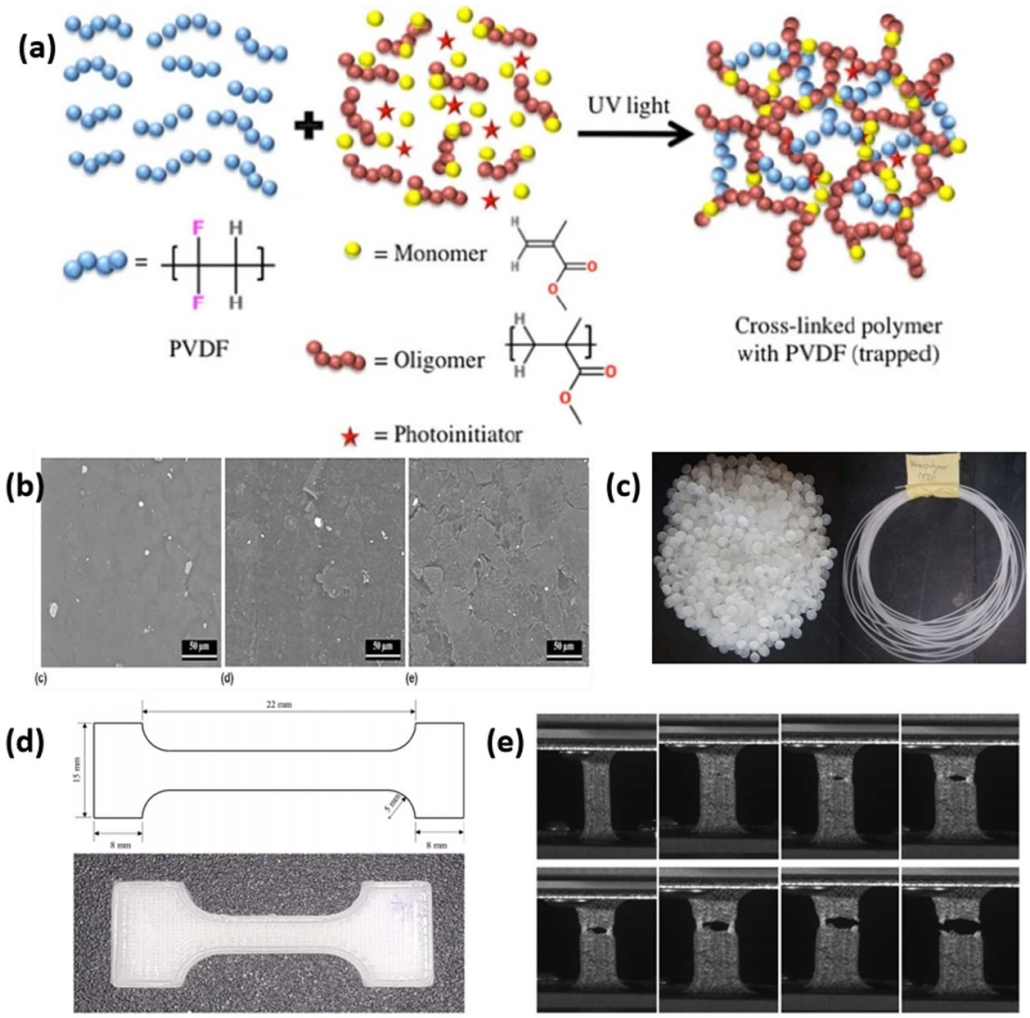

Figure 6. (a) Photopolymerization of the methacrylate monomer and oligomers along with the PVDF in DMF. (b) SEM images of 3D-printed PVDF surfaces as increasing concentration of PVDF with DMF dissolution treatment. Reprinted by permission from Springer Nature Customer Service Centre GmbH: [Springer Nature] [MRS Communications] [47], (2019). (c) Optical image of homopolymer PVDF resin pellets for 3D printing process. (d) 3D-printed PVDF sample for tensile test, and (e) tensile testing progression for 3D-printed PVDF. Reproduced with permission from [46]. [Emerald Publishing Limited].

and pyroelectric properties [65]. Hence, PVDF has been widely utilized in 3D printing to produce uniformly thin layers or films for device and sensor fabrication.

Similar to 3D printing for piezoceramics, PVDF can be produced using SLA. In representative work, PVDF powder was stirred and combined with photopolymer resin in N, N-Dimethylformamide (DMF) via a magnetic stirrer (figure 6(a)). Then an SLA 3D printer was used to photocure the mixed slurry to produce samples with 100 μm layer thickness [47]. Optimization of the 3D printing process focused on the weight ratio of PVDF to DMF in solution to disperse the PVDF molecular chains within the photopolymer resin homogeneously with the DMF solvent. As the weight ratio of PVDF to DMF solvent increased, the surface of the 3D-printed PVDF became coarser and more lacking in PVDF agglomerates. The defect was likely caused by precipitation polymerization of the PVDF within the photopolymer resin (figure 6(b)). Electrical poling was implemented using 3 MV m^{-1} applied voltage for 15 h at room temperature, and the piezoelectric coefficient (d_{31}) achieved was 0.014 pC N^{-1} with 2 wt% of PVDF/photopolymer resin. Another example showed that 3D-printed PVDF with multilayer has a higher piezoelectric coefficient of 130 pC N^{-1}. In other work, material extrusion AM (MEAM) was investigated for 3D-printed PVDF fabrication [46]. Homopolymer PVDF resin pellets (figure 6(c)) in wire form were extruded layer by layer via MEAM at an optimized temperature of 210 °C. The 3D-printed sample was used for tensile tests (figures 6(d) and (e)). The test results demonstrated promising mechanical properties. To improve upon the standard poling process which requires high voltage and long time period, PVDF-co-hexafluoropropylene (PVDF-HFP) was fabricated via a DLP printing process and an *in situ* poling system, The novel printing technique yielded a 10× reduction in the total processing time and a printed PVDF film with piezoelectric coefficient of 42 pC N^{-1} [105].

Currently, the piezoelectric properties of 3D-printed PVDF still need to be improved for it to be comparable to traditional piezoceramics. There are several 3D printing methods to

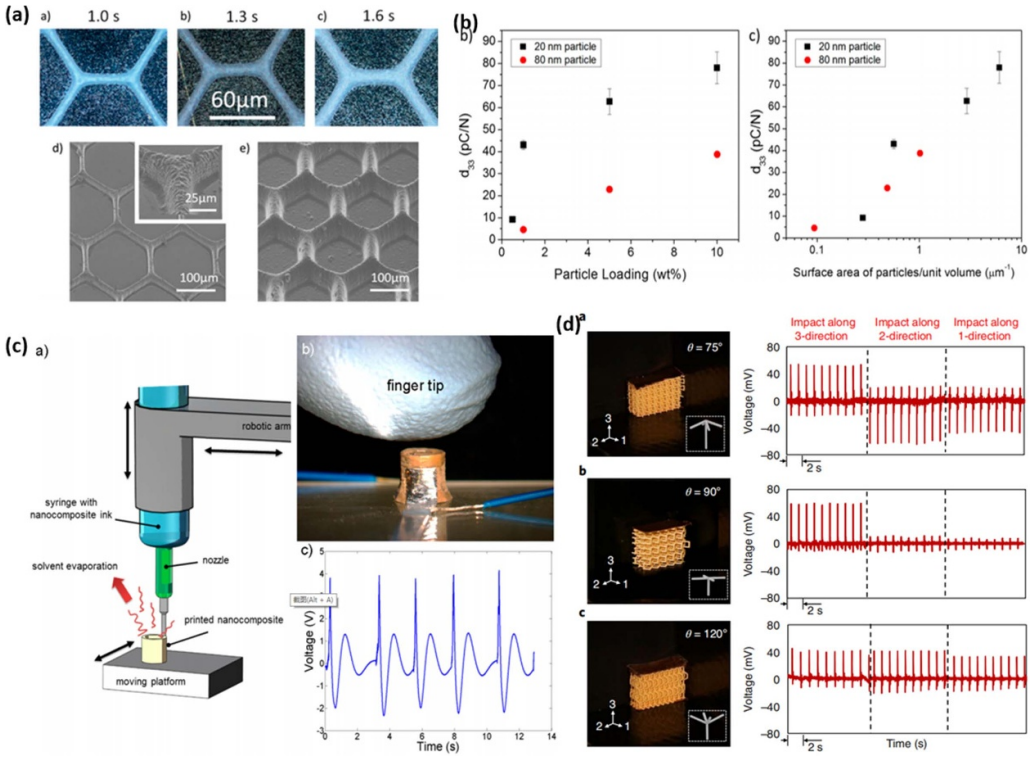

Figure 7. (a) Optical image and SEM image of 3D-printed structure during different exposure time. (b) Piezoelectric coefficients (d_{33}) as a function of particle loading percentage and surface area of particle/unit volume. Reprinted with permission from [111]. Copyright (2016) American Chemical Society. (c) 3D printing method for PVDF, optical image of the fabricated sensor and output of piezoelectric voltage during the finger-tap test. Reprinted with permission from [112]. Copyright (2017) American Chemical Society. (d) Optical images of printed PZT metamaterials and their voltage output during impact . Reprinted by permission from Springer Nature Customer Service Centre GmbH: [Springer Nature] [Nature Materials] [113], (2019).

produce PVDF. However, the selection of piezoelectric polymers utilized in 3D printing is still limited. Piezoelectric polymers, such as PLA or PVF, will be further studied in 3D printing processes for biomedical application.

3.3. *Piezoelectric composite*

Piezoelectric composite, comprised of more than two piezoelectric materials, contains piezoceramics and polymers as two-phase composites. This combination achieves superior piezoelectric properties and has generated significant research interest [106–108]. Specifically, composites that use a polymer with low permittivity can achieve improved voltage coefficient (g_{33}) due to a reduction in overall permittivity of the composite material [20, 93]. Composites can be categorized into ten different types (e.g. 2–2, or 1–3) according to their phase connectivity [16, 109, 110]. Combined with 3D printing, piezoelectric composites can be more easily fabricated with intricate structures and hold great potential in future investigation.

Kim *et al* illustrated the influence of surface modification and experimental conditions on the performance of 3D-printed (0–3) piezoelectric polymer nanocomposites [111]. Mixed with a functionalizing agent (TMSPM), BTO-nanoparticles suspended in a photocurable resin solution were cured via an UV light 3D printing system. The nanoparticles were then sealed into the matrix producing microscalar features when the photocurable resin was cross-linked under exposure to UV light. As shown in figure 7(a), structural variations can be constructed via tuning the UV exposure time. The use of larger nanoparticles restricts nanoparticle − polymer interactions and reduces stress-transfer efficiency. As shown in figure 7(b), functionalizing agent grafted onto smaller nanoparticles increased the stress-transfer efficiency, leading to enhancement of inorganic-polymer interfacial interaction. In this way, printed materials were poled at a voltage of 10.2 MV m^{-1} at 135 °C for 4 h, and decreasing the edge-length of nanoparticles causes an increase in piezoelectric coefficient ($d_{33} \sim 80$ pC N^{-1}).

In further work in this area, Bodkhe *et al* mixed BTO nanoparticles with printable PVDF by ball milling [112]. Excellent dielectric and piezoelectric properties ($d_{33} \sim 18$ pC N^{-1}) were achieved by fusion of the solvent evaporation-assisted 3D printing method due to the prevalence of β-phase PVDF polymer. A 3D-printed senor fabricated using this process was able to output up to 4 V without poling when stimulated by the tapping of a human finger (figure 7(c)). The work demonstrated a one-step 3D printing process for piezocomposites, opening new avenues of research in advanced sensor design. Cui *et al* reported using AM to fabricate PZT

nanocomposites with complex 3D architectures with arbitrary piezoelectric coefficient tensors [113]. This methodology is meant to improve the raw material's piezoelectric coefficients, which are restricted by the material's original crystal structure. As identical cyclic loading was utilized in each of the three orthogonal directions, three printed samples exhibited uniformly anisotropic response (figure 7(d)). The ability to fabricate these flexible 3D-printed PZT composite devices is promising for applications such as smart sensing and medical transducers.

4. Device and applications

4.1. Ultrasound devices

Ultrasonic devices have been widely utilized in biomedical devices, especially in energy harvesting and bioimaging, since they can be applied in a non-invasive manner [2, 8, 114, 115]. Generally, the essential components of the internal structure of ultrasonic devices include piezoelectric materials, which determines the device's performance in terms of sensitivity, electrical impedance, and bandwidth [2]. These parameters are critical to the optimization of the functionality of the device. New fabrication processes such as 3D printing hold promise in the ability to selectively optimize these different performance parameters and the fabrication of complex shapes. Therefore, 3D printing piezoelectric material has become an active area of research area [9].

Mask image projection-based stereolithography (MIP-SL) is one 3D printing method to realize ultrasonic devices [52]. BTO nano-powder was used to form complex geometrical structures with excellent piezoelectric constant (160 pC N^{-1}) and permittivity (1350) [52]. The 3D-printed devices were investigated for applications including ultrasonic sensing and energy focusing. Figure 8(a) shows representative structures, including a 64-pillar annular segment array as well as a concave piezoelectric element. These were fabricated using the MIP-SL process. The 3D-printed focused concave shape piezoelectric element (PF-CPE) was assembled into an ultrasound transducer housing to study its application to ultrasonic imaging (figure 8(b)). The measured electromechanical coupling factor (k_t) of the transducer was 0.474, and the magnitude of the peak to peak pulse-echo response of the printed transducer was 0.35 V (figure 8(c)). The line spread function resolution of the transducer was measured and found to be 240 μm in the axial direction and 770 μm in the lateral direction. The device was further used to image a porcine eyeball. The structure of the cornea and other constituent layers as imaged using the fabricated device are shown in figure 8(d) and demonstrate the potential utility of the printed focused transducer for ultrasonic imaging applications [52].

In other reported work with SLA, a 3D-printed BTO ceramic ultrasound transducer consisting of a focused ultrasonic array with 1.4 MHz center frequency, 40% fractional bandwidth and 50 dB insertion loss was realized by 3D printing BTO in optimized weight percentage. The pulse-echo response of the printed array had a peak to peak magnitude of 0.28 V, which is adequate to achieve reasonably sensitive ultrasonic imaging [116]. Chen *et al* demonstrated a 3D-printed annular piezoelectric array structure (figure 8(e)) to modify the acoustic beam and thereby improved spatial resolution in ultrasonic imaging applications [117]. The 3D-printed array transducer (figure 8(f)) demonstrated lateral resolution (beam width) less than 1.1 mm with a tunable focal depth from 5.6 mm to 8 mm. Moreover, Zeng *et al* used MIP-SL, to fabricate ultrasonic devices with complex honeycomb structures for ultrasonic sensing applications [20]. The 3D-printed BTO honeycomb structure can be used as a piezoelectric composite by adding low-permittivity epoxy. The fabricated device was encapsulated in silicone rubber, and a stand-alone ultrasound transducer was used to transmit ultrasonic energy directly to the printed honeycomb structure. The received ultrasound wave was converted to electrical signals with 180 mV_{pp} maximum value and 9 nW output power. Such 3D-printed structures with complex geometries are promising for wireless energy harvesting applications and merit further study.

4.2. Wearable devices

With the benefits of less weight, improved flexibility, and the ability to be easily worn on the human body, wearable electronic devices have played an essential role in biomedical monitoring, ranging from heart-rate sensing to cortisol sensing [118–122]. However, the utility of wearable devices is typically limited due to their power supply technology requirements [123]. Piezoelectric material can convert mechanical energy into electrical energy and therefore is potentially useful for energy harvesting for wearable devices [8, 123]. Therefore, integrating piezoelectric materials into future wearable devices for energy harvesting is potentially important for their development. Piezoceramics fabricated by traditional methods, such as tape casting, are typically stiff and limited to the realization of simple 2D structures. For convenient use in wearable applications on the human body, piezoelectric materials need to be flexible, stretchable, and fabricated with microscalar resolution. Microstructured piezoelectric materials are especially attractive because they can be connected and integrated to form a piezoelectric array interconnected using soft copper wire. Such microstructured arrays can enable more efficient energy harvesting in a more stretchable and flexible conformal surface mesh that is conveniently applied to the human body [9]. PVDF, with its natural flexibility, low acoustic impedance, and excellent chemical stability, is an important material to fabricate flexible energy harvesting structures in wearable devices [124–127]. 3D printing has advantages in producing piezoelectric materials, including rapid manufacturing while retaining the required piezoelectric properties of the material. Therefore, it has great potential for fabricating piezoelectric materials for use in wearable devices.

Recently, Yao *et al* demonstrated using 3D printing technology to fabricate a flexible PZT nanocomposite with high d_{33}, close to the theoretical upper bound [50]. The devices, which were robust and had high sensitivity, could be used as wearables for sensing incoming airflow pressure and were further integrated into gloves for impact absorption (figure 9(a)). To demonstrate high piezoelectric response, a mechanical shaker

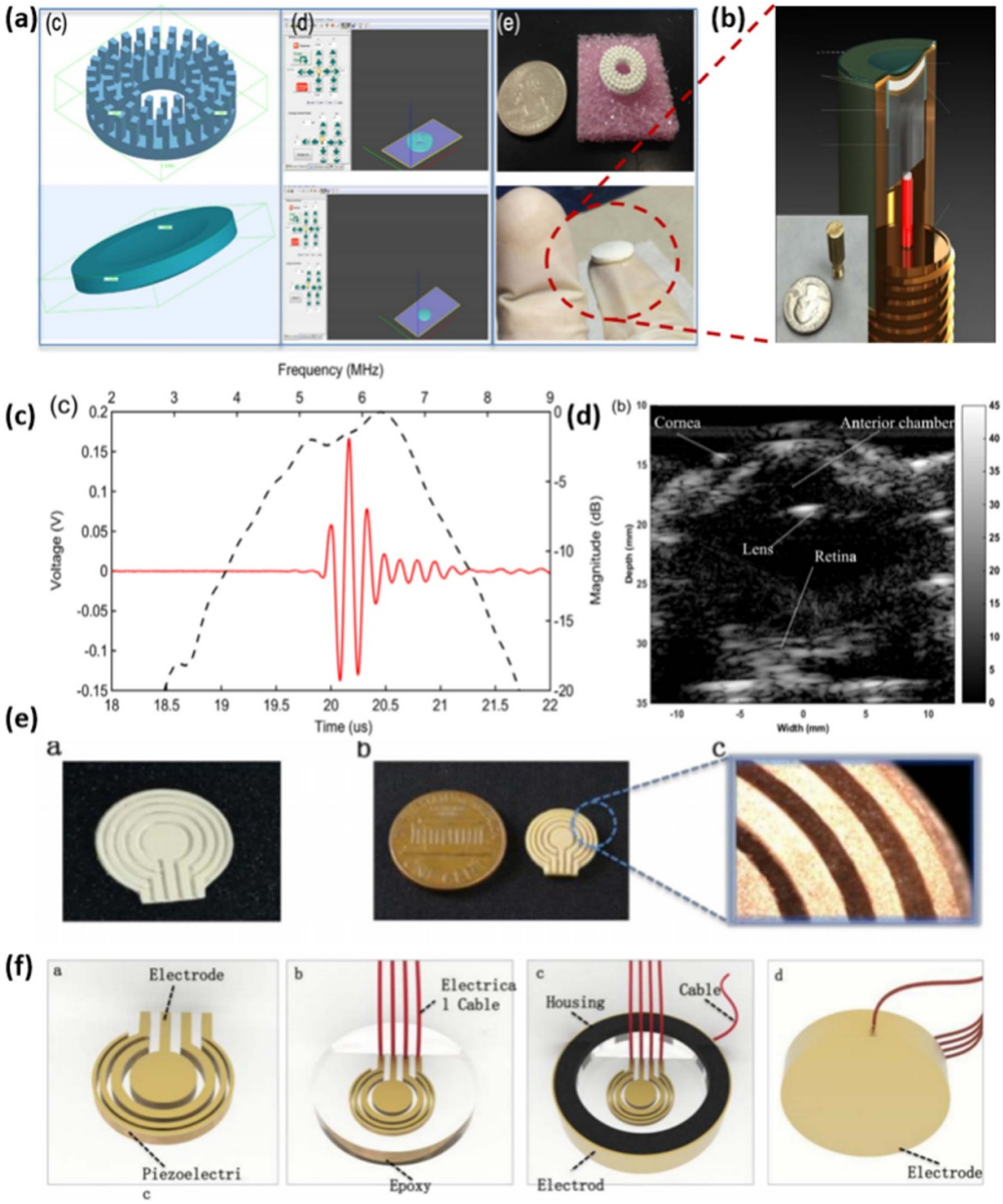

Figure 8. (a) Solidworks models and optical images of printed samples. (b) Structure of ultrasound transducer fabricated by 3D-printed pieces. (c) Pulse-echo performance of the fabricated transducer. (d) Ultrasonic imaging of the porcine eyeball gained by the transducer with 3D-printed sample. Reprinted from [52], Copyright (2016), with permission from Elsevier. (e) Green part and sintered sample of printed BTO annular array structure. (f) Structure of annular ultrasound array transducer integrated by a 3D-printed sample and electrical cables. Reproduced from [117]. CC BY 4.0.

with a sawtooth input waveform was applied to the device and used to generate an induced output voltage higher than that previously obtained using commercial PVDF (figure 9(b)). Inflow air pressure at a 90° angle of incidence produced the highest measured voltage (3 mV) (figure 9(c)). Therefore, wearables based on 3D-printed PZT nanocomposite can be responsive and able to sense data without the requirement of being encapsulated into sensor patches. In this way, 3D-printed nanocomposites are promising for use as flexible self-sensing materials and wearable devices.

In other work in this area, PVD-based flexible piezoelectric polymers were used to create piezoelectric energy harvesters (PEH) in the shape of a rugby ball (figure 9(d)) [45]. These energy harvesters were implemented using 3D-printed flexible multilayer b-phase PVDF-TrFE copolymer with high d_{33}. The vibration energy harvesting performance for multiple fabricated devices was compared by experiment for the following sample types: one-layer flat PEH (one-layer FPEH), six-layer FPEH, a single-layer a-PVDF flat PEH (one-layer a-FPEH), single-layer rugby ball-structured PEH (one-layer RPEH) and

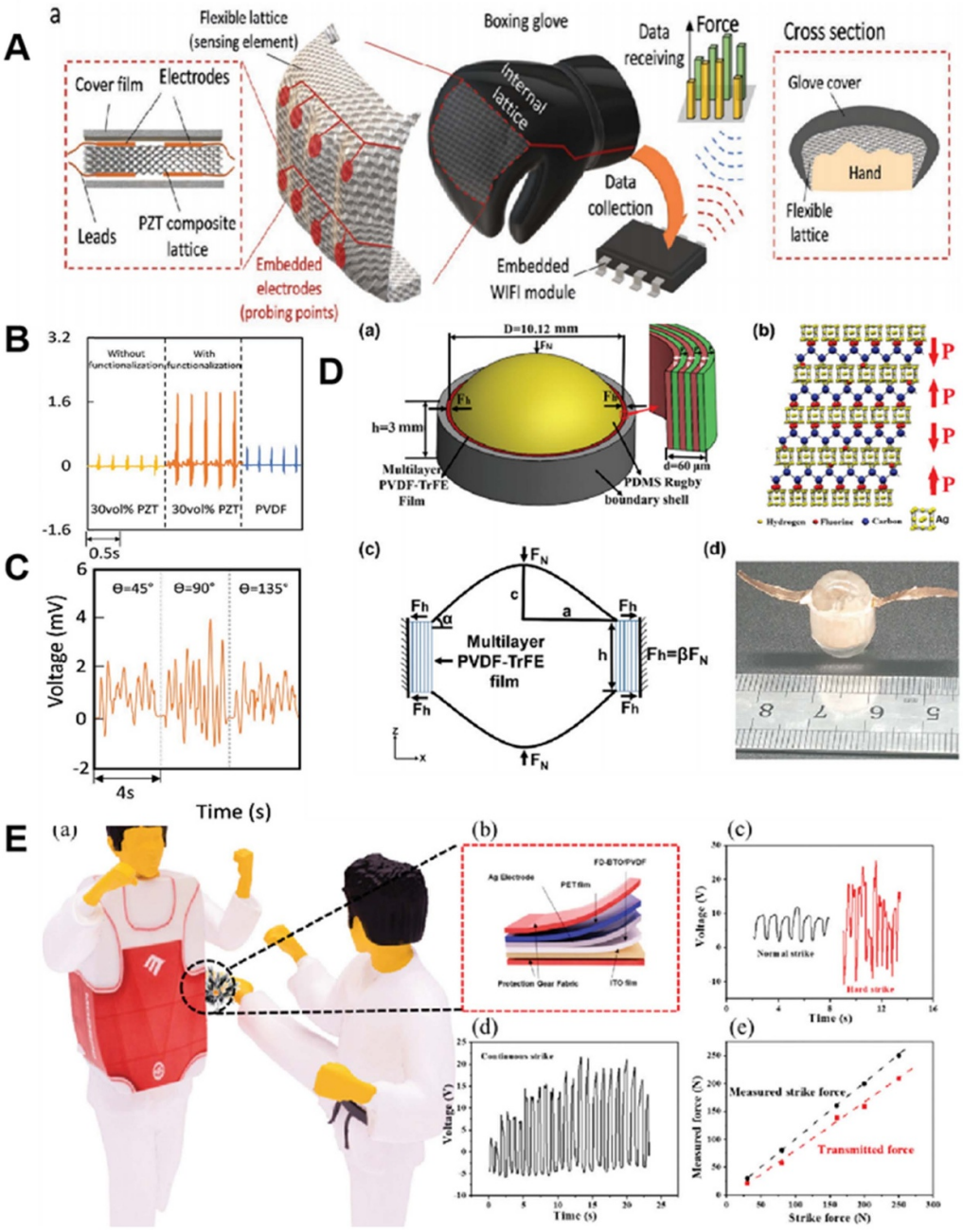

Figure 9. (a) Schematics of the self-sensing boxing glove integrated by printed composite. (b) Comparison of the voltage output of several samples. (c) Voltage output of the 3D-printed sensor as a function of time with airflow applied at various angles. [50] John Wiley & Sons. [Copyright © 2019 WILEY-VCH Verlag GmbH & Co. KGaA, Weinheim]. (d) Schematic diagrams of the rugby ball-shaped PEH, multilayer PVDF-TrFE and internal electrode layer. Reproduced from [45] with permission of The Royal Society of Chemistry. (e) Schematic of taekwondo sport with printed composite. Reproduced from [53] with permission of The Royal Society of Chemistry.

a six-layer RPEH. The results demonstrated that the six-layer RPEH device had the highest output voltage (88.62 V) and power density output (16.41 mW cm^{-2}) at 10 Hz. This excellent performance was due to the effect of the rugby ball structure. Furthermore, DC power created by rectifying the harvested AC voltage could charge a Li-ion battery and drive LEDs [45]. Therefore, using 3D printing allows for the manufacture of PEH devices in a timely manner with high power density. These features make this technique attractive as a potential way to satisfy the power needs for self-powered wearable electronics in future applications.

Additional work for 3D printing piezoelectric wearables was illustrated by Li *et al*, who fabricated a 3D-printed self-powered sensor based on hydrophobic surface-functionalized BTO/PVDF composite film [53]. Functionalization using perfluorodecyltriethoxysilane improved the interface bond

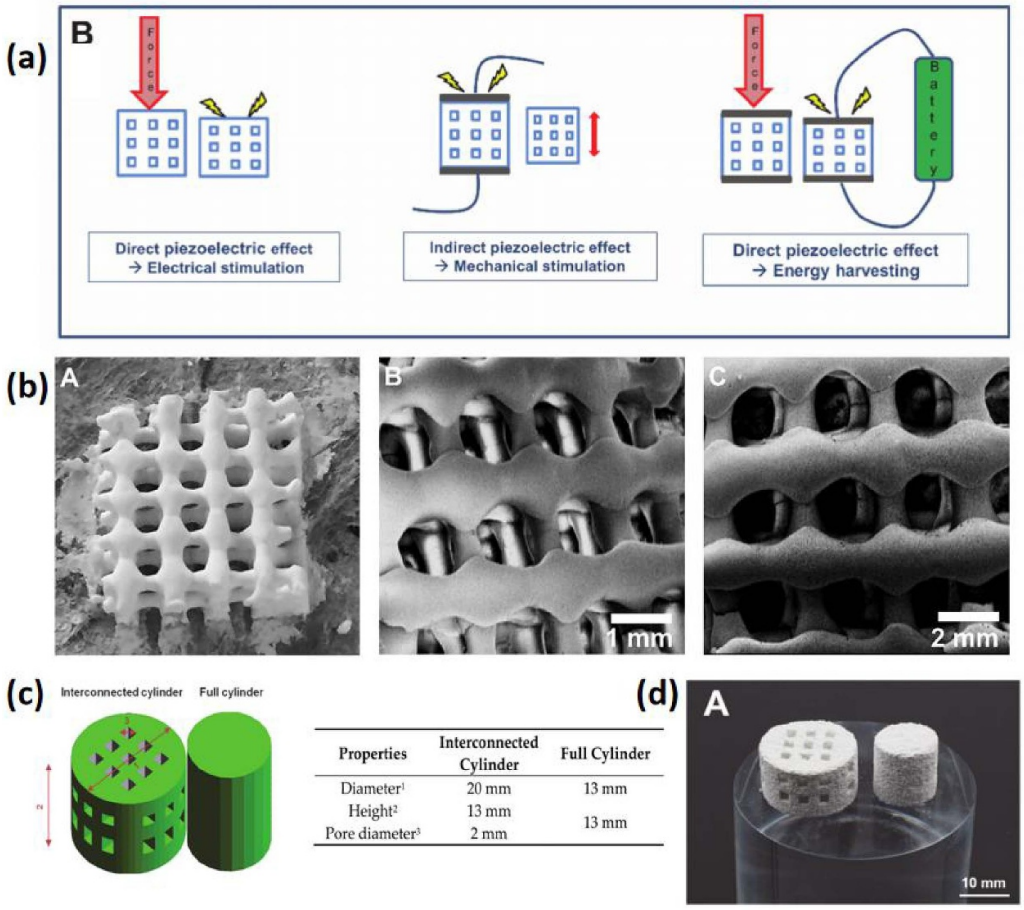

Figure 10. (a) Different piezoelectric effects for bone stimulation. (b) SEM of printed scaffolds. Reprinted from [131], Copyright (2019), with permission from Elsevier. (c) CAD model and parameters of composite scaffolds. (d) 3D-printed scaffolds before sintering. (a,c,d) Reproduced from [130]. CC BY 4.0.

between the BTO and PVDF, and increased the amount of β-phase PVDF in the composite. The improvement led to the fabricated sensors producing a 30 V output response to 500 kPa pressure input. The 3D-printed BTO/PVDF composite sensors were integrated into protective sports gear for Korean Taekwondo martial arts and used to monitor human movement (figure 9(e)). In experiments, the voltage generated by the resulting smart-sensor protective gear could be used to differentiate the magnitude of the striking force. The self-powered sensor array implemented using the 3D-printed BTO/PVDF sensors was able to convert input pressure to output electrical power, which was then used to monitor human motion and map motion patterns without a stand-alone energy source [53]. This same technique holds promise for use in harvesting biomechanical energy for standalone biomedical monitoring systems.

4.3. Bone devices

Piezoelectric effects in bone have been known and explored as far back as 1957 [6]. Since that early work, research on applications of piezoelectric materials in bone for regulating bone cell growth and regeneration has attracted significant attention [6, 128]. Piezoelectric materials with ferroelectric properties are able to control the interaction between ions and salts *in situ* to regulate the surface charge of biological materials in physiological environments. These effects are being explored for their potential to influence protein adhesion and bone regeneration [6, 128]. The piezoelectric properties of bone can induce self-healing by generating an electric signal from movement [6]. Implanted piezoelectric material scaffolds can create electric signals using dynamically harvested energy, enhancing the stimulus of bone cells and improving their attachment to the scaffolds [129]. There are two types of piezoelectric effect in bone stimulation (figure 10(a)): direct piezoelectric effect (piezoelectric implants for electrical stimulation or energy harvesting to supply other devices) and indirect piezoelectric effect (mechanical stimulation) [130]. Liu *et al* reported the use of porous titanium scaffolds with piezoelectric BTO coating to promote osteogenic differentiation based on the piezoelectric effect induced by low-intensity pulsed ultrasound stimulation [54]. 3D printing of piezoelectric materials is a promising technique for realizing intricate structures required to fabricate future bone stimulation implants, and smart stimulatory scaffolds.

Tariverdian *et al* demonstrated the fabrication of 3D-printed barium strontium titanate (BST)/β-tricalcium phosphate (β-TCP) composite scaffolds with interconnected macropores (figure 10(b)) [131]. These 3D-printed implantable materials were investigated for their ability to induce bioactive and piezoelectric activity for bone healing. The dielectric constant of the material was improved by increasing the BST phase fraction in the composite [131]. Optimized compressive strength (135 GPa), elasticity (1.83×10^6 MPa), and Young's modulus (157.24 MPa) were obtained with a composition of 60% BST/40% β-TCP in the fabricated samples. Moreover, the samples also showed optimized bone-like apatite formation in simulated body fluid, which implies an excellent ability to promote osteoblast growth and differentiation. Similarly, 3D-printed piezoelectric porous BTO and hydroxyapatite (HA) composite scaffolds with a d_{33} of 3 pC N^{-1}, outstanding cytocompatibility, and cell adhesion have also been designed and reported (figures 10(c) and (d)) [130]. MG-63 cell spreading, improved adhesion, and viability of mouse calvaria pre-osteoblast MC3T3-E1 cells on the 3D-printed scaffolds were observed. Therefore, the 3D-printed BTO/HA scaffold achieved cytocompatibility and is promising for use in osteoblast-like cell regeneration and adhesion [130].

Utilizing 3D printing methods to fabricate piezoelectric material applied in implant devices, such as scaffolds is considered a novel strategy for bone regeneration and engineering. Future work will concentrate on developing novel piezoelectric composite devices with excellent strength, biodegradability, and biocompatibility. At the same time, for optimized piezoelectric properties, active research on the selection of piezoelectric materials needs to be investigated.

5. Conclusion and outlook

In recent years, 3D printing technology has generated increasing interest in research, and is becoming an important tool in biomedical applications. This review summarized recent advances in 3D printing technology to manufacture piezoelectric devices for biomedical applications, including the printing process, material categories, and integrated devices. As explained in this review, 3D printable piezoelectric materials can be subdivided into piezoelectric ceramics, piezoactive polymers, and piezoelectric composites. Optimized 3D-printed piezoelectric composites are promising for their potential as the next generation of multi-functional devices with low-cost, high efficiency, and excellent performance.

In the future, with the increasing maturity of 3D printing technology, we expect that 3D-printed piezoelectric materials will contribute to biomedical fields in the following areas:

First, while applied 3D printing processes (e.g. SLA, SLS and FDM) can fabricate samples in a relatively short time, future development of advanced 3D-printing methods will significantly reduce the fabrication time while still retaining the superior performance of piezoelectric materials. For example, in the future, novel nano-printing technology will be more widely available and used in customized designs to manufacture smart structures. This new manufacturing method is poised to greatly facilitate the fabrication of miniaturized and complex piezoceramic structures (e.g. metamaterials and biomimetic structures) while maintaining desirable performance in highly integrated devices and systems. In addition, recent advances in multi-material 3D and four-dimensional printing (with time as the fourth dimension) show that this technology can extend the design space further beyond complex geometries and expand to the printing of metamaterials with complex functionality.

The second important aspect where 3D printing will contribute to future biomedical systems is to broaden the selection of suitable piezoelectric materials. This development will free up the field from the limitations of the current printable piezoelectric materials (e.g. BTO, PZT, and KNN). 3D-printing technology with higher printing resolution needs to be investigated to fabricate microscale or even nanoscale piezoelectric devices with multimaterial fabrication capability. Future 3D-printable piezoelectric materials will be novel piezoelectric composites with improved performance properties such as higher piezoelectric or ferroelectric characteristics, more complex 3D-geometric shapes, bio-non-toxicity, and even biodegradability for various biomedical applications. New materials with these improved characteristics are in demand for next-generation implantable biomedical devices.

The last significant area for future development of 3D-printed biomedical materials and devices is in overall system integration with electronics and targeting specific biomedical applications. Highly integrated and autonomous biomedical sensing applications, such as wireless implants and wearable biomonitoring systems, will benefit from high-performance piezoelectric materials, especially piezoceramics with microscale structure and flexibility. These highly integrated and adapted sensing systems will achieve their monitoring goals while maintaining reduced impact on human health and regular movement. Signal actuation and transmission chips can also be integrated into these complex printed systems to achieve diverse uses and functions beyond current biomedical applications. Example applications for these smart material systems include implantable/wearable devices for healthcare and motion monitoring, portable/mobile electronic devices for wireless power harvesting and data transmission, home automation for switches and smart metering, and intelligent automobile systems for machine health monitoring and wireless sensing.

Data availability statement

No new data were created or analysed in this study.

ORCID iDs

Yushun Zeng https://orcid.org/0000-0001-5995-4085
Laiming Jiang https://orcid.org/0000-0002-8658-3168
Robert Wodnicki https://orcid.org/0000-0002-3853-4433
Yong Chen https://orcid.org/0000-0002-8377-5914

References

[1] Chen R *et al* 2018 Eco-friendly highly sensitive transducers based on a new KNN–NTK–FM lead-free piezoelectric ceramic for high-frequency biomedical ultrasonic imaging applications *IEEE Trans. Biomed. Eng.* **66** 1580–7

[2] Jiang L, Chen R, Xing J, Lu G, Li R, Jiang Y, Kirk Shung K, Zhu J and Zhou Q 2019 Fabrication of a (K, Na) NbO_3-based lead-free 1–3 piezocomposite for high-sensitivity ultrasonic transducers application *J. Appl. Phys.* **125** 214501

[3] Covaci C and Gontean A 2020 Piezoelectric energy harvesting solutions: a review *Sensors* **20** 3512

[4] Sezer N and Koç M 2020 A comprehensive review on the state-of-the-art of piezoelectric energy harvesting *Nano Energy* **80** 105567

[5] Chen C, Sharafi A and Sun J-Q 2020 A high density piezoelectric energy harvesting device from highway traffic–design analysis and laboratory validation *Appl. Energy* **269** 115073

[6] Tandon B, Blaker J J and Cartmell S H 2018 Piezoelectric materials as stimulatory biomedical materials and scaffolds for bone repair *Acta Biomater.* **73** 1–20

[7] Jiang L, Lu G, Yang Y, Zeng Y, Sun Y, Li R, Humayun M S, Chen Y and Zhou Q 2021 Photoacoustic and piezo-ultrasound hybrid-induced energy transfer for 3D twining wireless multifunctional implants *Energy Environ. Sci.* **14** 1490–505

[8] Jiang L, Yang Y, Chen Y and Zhou Q 2020 Ultrasound-induced wireless energy harvesting: from materials strategies to functional applications *Nano Energy* **77** 105131

[9] Jiang L *et al* 2019 Flexible piezoelectric ultrasonic energy harvester array for bio-implantable wireless generator *Nano Energy* **56** 216–24

[10] Priya S *et al* 2019 A review on piezoelectric energy harvesting: materials, methods, and circuits *Energy Harvest. Syst.* **4** 3–39

[11] Jantunen H, Hu T, Uusimäki A and Leppävuori S 2004 Tape casting of ferroelectric, dielectric, piezoelectric and ferromagnetic materials *J. Eur. Ceram. Soc.* **24** 1077–81

[12] Wang J, Chen M, Zhao X, Wang F, Tang Y, Lin D and Luo H 2021 Fabrication and high acoustic performance of high frequency needle ultrasound transducer with PMN-PT/epoxy 1–3 piezoelectric composite prepared by dice and fill method *Sens. Actuators* A **318** 112528

[13] Mirza M S, Liu Q, Yasin T, Qi X, Li J-F and Ikram M 2016 Dice-and-fill processing and characterization of microscale and high-aspect-ratio (K, Na) NbO_3-based 1–3 lead-free piezoelectric composites *Ceramics Int.* **42** 10745–50

[14] Liu H, Gao Y, Ding S, Peng F and Zhu D 2019 Research on the effect of the waveform on the droplet injection behavior of a piezoelectric print head and the forming accuracy of casting sand molds *Int. J. Adv. Manuf. Technol.* **100** 251–61

[15] Mirzazadeh Z, Sherafat Z and Bagherzadeh E 2021 Physical and mechanical properties of PVDF/KNN composite produced via hot compression molding *Ceramics Int.* **47** 6211–9

[16] Chen C, Wang X, Wang Y, Yang D, Yao F, Zhang W, Wang B, Sewvandi G A, Yang D and Hu D 2020 Additive manufacturing of piezoelectric materials *Adv. Funct. Mater.* **30** 2005141

[17] Zou X-Y, Chen Q, Liang B and Cheng J-C 2007 Control of the elastic wave bandgaps in two-dimensional piezoelectric periodic structures *Smart Mater. Struct.* **17** 015008

[18] Nguyen-Xuan H, Liu G, Nguyen-Thoi T and Nguyen-Tran C 2009 An edge-based smoothed finite element method for analysis of two-dimensional piezoelectric structures *Smart Mater. Struct.* **18** 065015

[19] Yoon Y-J, Moon S K and Hwang J 2014 3D printing as an efficient way for comparative study of biomimetic structures—trabecular bone and honeycomb *J. Mech. Sci. Technol.* **28** 4635–40

[20] Zeng Y *et al* 2020 3D-printing piezoelectric composite with honeycomb structure for ultrasonic devices *Micromachines* **11** 713

[21] Bodkhe S and Ermanni P 2019 Challenges in 3D printing of piezoelectric materials *Multifunct. Mater.* **2** 022001

[22] Espera A H, Dizon J R C, Chen Q and Advincula R C 2019 3D-printing and advanced manufacturing for electronics *Progress Addit. Manuf.* **4** 245–67

[23] Song X, Chen Z, Lei L, Shung K, Zhou Q and Chen Y 2017 Piezoelectric component fabrication using projection-based stereolithography of barium titanate ceramic suspensions *Rapid Prototyp. J.* **23** 44–53

[24] Yang Y, Li X, Zheng X, Chen Z, Zhou Q and Chen Y 2018 3D-printed biomimetic super-hydrophobic structure for microdroplet manipulation and oil/water separation *Adv. Mater.* **30** 1704912

[25] Yang Y, Li X, Chu M, Sun H, Jin J, Yu K, Wang Q, Zhou Q and Chen Y 2019 Electrically assisted 3D printing of nacre-inspired structures with self-sensing capability *Sci. Adv.* **5** eaau9490

[26] Song X, Chen Y, Lee T W, Wu S and Cheng L 2015 Ceramic fabrication using mask-image-projection-based stereolithography integrated with tape-casting *J. Manuf. Process.* **20** 456–64

[27] Yang Y, Chen Z, Song X, Zhang Z, Zhang J, Shung K K, Zhou Q and Chen Y 2017 Biomimetic anisotropic reinforcement architectures by electrically assisted nanocomposite 3D printing *Adv. Mater.* **29** 1605750

[28] Yang Y, Song X, Li X, Chen Z, Zhou C, Zhou Q and Chen Y 2018 Recent progress in biomimetic additive manufacturing technology: from materials to functional structures *Adv. Mater.* **30** 1706539

[29] Skowyra J, Pietrzak K and Alhnan M A 2015 Fabrication of extended-release patient-tailored prednisolone tablets via fused deposition modelling (FDM) 3D printing *Eur. J. Pharm. Sci.* **68** 11–17

[30] Kim H and Lee S 2020 Characterization of electrical heating of graphene/PLA honeycomb structure composite manufactured by CFDM 3D printer *Fashion Textiles* **7** 1–18

[31] Yang H, Lim J C, Liu Y, Qi X, Yap Y L, Dikshit V, Yeong W Y and Wei J 2017 Performance evaluation of projet multi-material jetting 3D printer *Virtual Phys. Prototy.* **12** 95–103

[32] Wang J, Goyanes A, Gaisford S and Basit A W 2016 Stereolithographic (SLA) 3D printing of oral modified-release dosage forms *Int. J. Pharm.* **503** 207–12

[33] Guerin S, Tofail S A and Thompson D 2019 Organic piezoelectric materials: milestones and potential *NPG Asia Mater.* **11** 1–5

[34] You Y-M *et al* 2017 An organic-inorganic perovskite ferroelectric with large piezoelectric response *Sci. Adv.* **357** 306–9

[35] Shin D-M, Hong S W and Hwang Y-H 2020 Recent advances in organic piezoelectric biomaterials for energy and biomedical applications *Nanomaterials* **10** 123

[36] Lee H S *et al* 2014 Flexible inorganic piezoelectric acoustic nanosensors for biomimetic artificial hair cells *Adv. Funct. Mater.* **24** 6914–21

[37] Jella V *et al* 2019 A comprehensive review of flexible piezoelectric generators based on organic-inorganic metal halide perovskites *Nano Energy* **57** 74–93

[38] Wang Z, Yuan X, Yang J, Huan Y, Gao X, Li Z, Wang H and Dong S 2020 3D-printed flexible, Ag-coated PNN-PZT ceramic-polymer grid-composite for electromechanical energy conversion *Nano Energy* **73** 104737

[39] Thuau D, Kallitsis K, Dos Santos F D and Hadziioannou G 2017 All inkjet-printed piezoelectric electronic devices: energy generators, sensors and actuators *J. Mater. Chem.* C **5** 9963–6

[40] Kuscer D, Drnovšek S and Levassort F 2021 Inkjet-printing-derived lead-zirconate-titanate-based thick films for printed electronics *Mater. Des.* **198** 109324

[41] Kozioł M, Szperlich P, Toroń B, Olesik P and Jesionek M 2020 Assessment of the piezoelectric response of an epoxy resin/SbSI nanowires composite filling FDM printed grid *Materials* **13** 5281

[42] Kim H, Fernando T, Li M, Lin Y and Tseng T-L B 2018 Fabrication and characterization of 3D printed $BaTiO_3$/PVDF nanocomposites *J. Compos. Mater.* **52** 197–206

[43] Qi F, Chen N and Wang Q 2017 Preparation of PA11/$BaTiO_3$ nanocomposite powders with improved processability, dielectric and piezoelectric properties for use in selective laser sintering *Mater. Des.* **131** 135–43

[44] Wang W, Sun J, Guo B, Chen X, Ananth K P and Bai J 2020 Fabrication of piezoelectric nano-ceramics via stereolithography of low viscous and non-aqueous suspensions *J. Eur. Ceram. Soc.* **40** 682–8

[45] Yuan X, Gao X, Yang J, Shen X, Li Z, You S, Wang Z and Dong S 2020 The large piezoelectricity and high power density of a 3D-printed multilayer copolymer in a rugby ball-structured mechanical energy harvester *Energy Environ. Sci.* **13** 152–61

[46] Momenzadeh N, Miyanaji H, Porter D A and Berfield T A 2020 Polyvinylidene fluoride (PVDF) as a feedstock for material extrusion additive manufacturing *Rapid Prototyp. J.* **26** 156–63

[47] Kim H, Manriquez L C D, Islam M T, Chavez L A, Regis J E, Ahsan M A, Noveron J C, Tseng T-L B and Lin Y 2019 3D printing of polyvinylidene fluoride/photopolymer resin blends for piezoelectric pressure sensing application using the stereolithography technique *MRS Commun.* **9** 1115–23

[48] Chen Y, Bao X, Wong C-M, Cheng J, Wu H, Song H, Ji X and Wu S 2018 PZT ceramics fabricated based on stereolithography for an ultrasound transducer array application *Ceramics Int.* **44** 22725–30

[49] Bach M, Sebastian T, Melnykowycz M, Lusiola T, Scharf D and Clemens F 2017 Additive manufacturing of piezoelectric 3–3 composite structures *Int. Conf. on Additive Manufacturing in Products and Applications* (Springer) pp 93–103

[50] Yao D *et al* 2019 Achieving the upper bound of piezoelectric response in tunable, wearable 3D printed nanocomposites *Adv. Funct. Mater.* **29** 1903866

[51] Chen W, Wang F, Yan K, Zhang Y and Wu D 2019 Micro-stereolithography of KNN-based lead-free piezoceramics *Ceramics Int.* **45** 4880–5

[52] Chen Z *et al* 2016 3D printing of piezoelectric element for energy focusing and ultrasonic sensing *Nano Energy* **27** 78–86

[53] Li H, Song H, Long M, Saeed G and Lim S 2021 Mortise–tenon joint structured hydrophobic surface-functionalized barium titanate/polyvinylidene fluoride nanocomposites for printed self-powered wearable sensors *Nanoscale* **13** 2542–55

[54] Liu W *et al* 2020 Fabrication of piezoelectric porous $BaTiO_3$ scaffold to repair large segmental bone defect in sheep *J. Biomater. Appl.* **35** 544–52

[55] Wickramasinghe S, Do T and Tran P 2020 FDM-based 3D printing of polymer and associated composite: a review on mechanical properties, defects and treatments *Polymers* **12** 1529

[56] Vyavahare S, Teraiya S, Panghal D and Kumar S 2020 Fused deposition modelling: a review *Rapid Prototyp. J.* **26** 176–201

[57] Kim H, Torres F, Wu Y, Villagran D, Lin Y and Tseng T-L B 2017 Integrated 3D printing and corona poling process of PVDF piezoelectric films for pressure sensor application *Smart Mater. Struct.* **26** 085027

[58] Przekop R E, Kujawa M, Pawlak W, Dobrosielska M, Sztorch B and Wieleba W 2020 Graphite modified polylactide (PLA) for 3D printed (FDM/FFF) sliding elements *Polymers* **12** 1250

[59] Popescu D, Zapciu A, Amza C, Baciu F and Marinescu R 2018 FDM process parameters influence over the mechanical properties of polymer specimens: a review *Polym. Test.* **69** 157–66

[60] Dave H K, Prajapati A R, Rajpurohit S R, Patadiya N H and Raval H K 2020 Investigation on tensile strength and failure modes of FDM printed part using in-house fabricated PLA filament *Adv. Mater. Process. Technol.* 1–22

[61] Dave H K, Patadiya N H, Prajapati A R and Rajpurohit S R 2019 Effect of infill pattern and infill density at varying part orientation on tensile properties of fused deposition modeling-printed poly-lactic acid part *Proc. Inst. Mech. Eng.* C **235** 1811–27

[62] Esslinger S, Grebhardt A, Jaeger J, Kern F, Killinger A, Bonten C and Gadow R 2021 Additive manufacturing of β-tricalcium phosphate components via fused deposition of ceramics (FDC) *Materials* **14** 156

[63] Janek M *et al* 2020 Mechanical testing of hydroxyapatite filaments for tissue scaffolds preparation by fused deposition of ceramics *J. Eur. Ceram. Soc.* **40** 4932–8

[64] Conzelmann N A, Gorjan L, Sarraf F, Poulikakos L D, Partl M N, Müller C R and Clemens F J 2020 Manufacturing complex Al_2O_3 ceramic structures using consumer-grade fused deposition modelling printers *Rapid Prototyp. J.* **26** 1035–48

[65] Liu X, Shang Y, Zhang J and Zhang C 2021 Ionic liquid-assisted 3D printing of self-polarized β-PVDF for flexible piezoelectric energy harvesting *ACS Appl. Mater. Interfaces* **13** 14334–41

[66] Long J, Gholizadeh H, Lu J, Bunt C and Seyfoddin A 2017 Application of fused deposition modelling (FDM) method of 3D printing in drug delivery *Curr. Pharm. Des.* **23** 433–9

[67] Melchels F P, Feijen J and Grijpma D W 2010 A review on stereolithography and its applications in biomedical engineering *Biomaterials* **31** 6121–30

[68] Borrello J, Nasser P, Iatridis J C and Costa K D 2018 3D printing a mechanically-tunable acrylate resin on a commercial DLP-SLA printer *Addit. Manuf.* **23** 374–80

[69] Zhang D, Liu X and Qiu J 2020 3D printing of glass by additive manufacturing techniques: a review *Front. Optoelectron.* 1–15

[70] Yun J S, Park T-W, Jeong Y H and Cho J H 2016 Development of ceramic-reinforced photopolymers for SLA 3D printing technology *Appl. Phys.* A **122** 1–6

[71] Mu Q, Wang L, Dunn C K, Kuang X, Duan F, Zhang Z, Qi H J and Wang T 2017 Digital light processing 3D

printing of conductive complex structures *Addit. Manuf.* **18** 74–83
[72] Patel D K, Sakhaei A H, Layani M, Zhang B, Ge Q and Magdassi S 2017 Highly stretchable and UV curable elastomers for digital light processing based 3D printing *Adv. Mater.* **29** 1606000
[73] Hwa L C, Rajoo S, Noor A M, Ahmad N and Uday M 2017 Recent advances in 3D printing of porous ceramics: a review *Curr. Opin. Solid State Mater. Sci.* **21** 323–47
[74] Hinczewski C, Corbel S and Chartier T 1998 Ceramic suspensions suitable for stereolithography *J. Eur. Ceram. Soc.* **18** 583–90
[75] Chu T-M G, Orton D G, Hollister S J, Feinberg S E and Halloran J W 2002 Mechanical and *in vivo* performance of hydroxyapatite implants with controlled architectures *Biomaterials* **23** 1283–93
[76] Fina F, Goyanes A, Gaisford S and Basit A W 2017 Selective laser sintering (SLS) 3D printing of medicines *Int. J. Pharm.* **529** 285–93
[77] Msallem B, Sharma N, Cao S, Halbeisen F S, Zeilhofer H-F and Thieringer F M 2020 Evaluation of the dimensional accuracy of 3D-printed anatomical mandibular models using FFF, SLA, SLS, MJ, and BJ printing technology *J. Clin. Med.* **9** 817
[78] Guo D, Li L T, Cai K, Gui Z I and Nan C W 2004 Rapid prototyping of piezoelectric ceramics via selective laser sintering and gelcasting *J. Am. Ceram. Soc.* **87** 17–22
[79] Rollo G *et al* 2020 On the synergistic effect of multi-walled carbon nanotubes and graphene nanoplatelets to enhance the functional properties of SLS 3D-printed elastomeric structures *Polymers* **12** 1841
[80] Campbell C G, Astorga D J, Martinez E and Celina M 2021 Selective laser sintering (SLS)-printable thermosetting resins via controlled conversion *MRS Commun.* **11** 173–8
[81] Si L, Han Y, Zhou M and Li M 2021 The influence of process parameters on the performance of nylon 6 selective laser sintering parts *J. Phys. Conf. Ser.* **1798** 012021
[82] Rosenthal W S *et al* 2020 "Sintering" models and *in-situ* experiments: data assimilation for microstructure prediction in SLS additive manufacturing of nylon components *MRS Adv.* **5** 1593–601
[83] Bochnia J and Blasiak S 2020 Stress relaxation and creep of a polymer-aluminum composite produced through selective laser sintering *Polymers* **12** 830
[84] Zhang Z, Yao X and Ge P 2020 Phase-field-model-based analysis of the effects of powder particle on porosities and densities in selective laser sintering additive manufacturing *Int. J. Mech. Sci.* **166** 105230
[85] Shao W, Wang Q, Wang F and Chen Y 2006 The cutting of multi-walled carbon nanotubes and their strong interfacial interaction with polyamide 6 in the solid state *Carbon* **44** 2708–14
[86] Ratsimba A, Zerrouki A, Tessier-Doyen N, Nait-Ali B, André D, Duport P, Neveu A, Tripathi N, Francqui F and Delaizir G 2021 Densification behaviour and three-dimensional printing of Y_2O_3 ceramic powder by selective laser sintering *Ceramics Int.* **47** 7465–74
[87] Yang Y, Peng S, Qi F, Zan J, Liu G, Zhao Z and Shuai C 2020 Graphene-assisted barium titanate improves piezoelectric performance of biopolymer scaffold *Mater. Sci. Eng.* C **116** 111195
[88] Liang Y, Zhao J, Huang Q, Hu P and Xiao C 2021 PVDF fiber membrane with ordered porous structure via 3D printing near field electrospinning *J. Memb. Sci.* **618** 118709
[89] Reiser A, Lindén M, Rohner P, Marchand A, Galinski H, Sologubenko A S, Wheeler J M, Zenobi R, Poulikakos D and Spolenak R 2019 Multi-metal electrohydrodynamic redox 3D printing at the submicron scale *Nat. Commun.* **10** 1–8
[90] Cooperstein I, Sachyani-Keneth E, Shukrun-Farrell E, Rosental T, Wang X, Kamyshny A and Magdassi S 2018 Hybrid materials for functional 3D printing *Adv. Mater. Interfaces* **5** 1800996
[91] Khoo Z X, Teoh J E M, Liu Y, Chua C K, Yang S, An J, Leong K F and Yeong W Y 2015 3D printing of smart materials: a review on recent progresses in 4D printing *Virtual Phys. Prototyp.* **10** 103–22
[92] Lee D H and Derby B 2004 Preparation of PZT suspensions for direct ink jet printing *J. Eur. Ceram. Soc.* **24** 1069–72
[93] Jiang L *et al* 2019 Ultrasound-induced wireless energy harvesting for potential retinal electrical stimulation application *Adv. Funct. Mater.* **29** 1902522
[94] Panda P 2009 Environmental friendly lead-free piezoelectric materials *J. Mater. Sci.* **44** 5049–62
[95] Wei H *et al* 2018 An overview of lead-free piezoelectric materials and devices *J. Mater. Chem.* C **6** 12446–67
[96] Kim K, Zhu W, Qu X, Aaronson C, McCall W R, Chen S and Sirbuly D J 2014 3D optical printing of piezoelectric nanoparticle–polymer composite materials *ACS Nano* **8** 9799–806
[97] Rosental T and Magdassi S 2019 A new approach to 3D printing dense ceramics by ceramic precursor binders *Adv. Eng. Mater.* **21** 1900604
[98] Wei X, Liu Y, Zhao D and Ge S S 2020 3D printing of piezoelectric barium titanate with high density from milled powders *J. Eur. Ceram. Soc.* **40** 5423–30
[99] Lewis J 2006 Material challenge for flexible organic devices *Mater. Today* **9** 38–45
[100] Liu Y, He K, Chen G, Leow W R and Chen X 2017 Nature-inspired structural materials for flexible electronic devices *Chem. Rev.* **117** 12893–941
[101] Lu L, Ding W, Liu J and Yang B 2020 Flexible PVDF based piezoelectric nanogenerators *Nano Energy* **78** 105251
[102] Sukumaran S, Chatbouri S, Rouxel D, Tisserand E, Thiebaud F and Tarak B Z 2020 Recent advances in flexible PVDF based piezoelectric polymer devices for energy harvesting applications *J. Intell. Mater. Syst. Struct.* **32** 746–80
[103] Jurczuk K, Galeski A, Mackey M, Hiltner A and Baer E 2015 Orientation of PVDF α and γ crystals in nanolayered films *Colloid Polym. Sci.* **293** 1289–97
[104] Li L, Zhang M, Rong M and Ruan W 2014 Studies on the transformation process of PVDF from α to β phase by stretching *RSC Adv.* **4** 3938–43
[105] Song H, Li H and Lim S J 2021 Fast 3D digital light process printing of PVDF-HFP composite with electric *in situ* poling system for piezoelectric applications *Macromol. Mater. Eng.* 2100266
[106] Aleshin V, Tsikhotsky E and Yatsenko V 2004 Prediction of the properties of two-phase composites with a piezoactive component *Tech. Phys.* **49** 61–66
[107] Qin Q-H 2004 Material properties of piezoelectric composites by BEM and homogenization method *Compos. Struct.* **66** 295–9
[108] Labusch M, Schröder J and Lupascu D C 2019 A two-scale homogenization analysis of porous magneto-electric two-phase composites *Arch. Appl. Mech.* **89** 1123–40
[109] Narita F and Fox M 2018 A review on piezoelectric, magnetostrictive, and magnetoelectric materials and device technologies for energy harvesting applications *Adv. Eng. Mater.* **20** 1700743
[110] Ting R Y 1992 A review on the development of piezoelectric composites for underwater acoustic transducer applications *IEEE Trans. Instrum. Meas.* **41** 64–67

[111] Kim K, Middlebrook J L, Chen J E, Zhu W, Chen S and Sirbuly D J 2016 Tunable surface and matrix chemistries in optically printed (0–3) piezoelectric nanocomposites *ACS Appl. Mater. Interfaces* **8** 33394–8
[112] Bodkhe S, Turcot G, Gosselin F P and Therriault D 2017 One-step solvent evaporation-assisted 3D printing of piezoelectric PVDF nanocomposite structures *ACS Appl. Mater. Interfaces* **9** 20833–42
[113] Cui H, Hensleigh R, Yao D, Maurya D, Kumar P, Kang M G, Priya S and Zheng X 2019 Three-dimensional printing of piezoelectric materials with designed anisotropy and directional response *Nat. Mater.* **18** 234–41
[114] Shi Q, Wang T, Kobayashi T and Lee C 2016 Investigation of geometric design in piezoelectric microelectromechanical systems diaphragms for ultrasonic energy harvesting *Appl. Phys. Lett.* **108** 193902
[115] Ilkhechi A K, Ceroici C, Dew E and Zemp R 2021 Transparent capacitive micromachined ultrasound transducer linear arrays for combined realtime optical and ultrasonic imaging *Opt. Lett.* **46** 1542–5
[116] Cheng J, Chen Y, Wu J-W, Ji X-R and Wu S-H 2019 3D printing of BaTiO3 piezoelectric ceramics for a focused ultrasonic array *Sensors* **19** 4078
[117] Chen Z, Qian X, Song X, Jiang Q, Huang R, Yang Y, Li R, Shung K, Chen Y and Zhou Q 2019 Three-dimensional printed piezoelectric array for improving acoustic field and spatial resolution in medical ultrasonic imaging *Micromachines* **10** 170
[118] Wang X, Liu Z and Zhang T 2017 Flexible sensing electronics for wearable/attachable health monitoring *Small* **13** 1602790
[119] Bent B, Goldstein B A, Kibbe W A and Dunn J P 2020 Investigating sources of inaccuracy in wearable optical heart rate sensors *npj Digit. Med.* **3** 1–9
[120] Kwak Y H, Kim W, Park K B, Kim K and Seo S 2017 Flexible heartbeat sensor for wearable device *Biosens. Bioelectron.* **94** 250–5
[121] Parlak O, Keene S T, Marais A, Curto V F and Salleo A 2018 Molecularly selective nanoporous membrane-based wearable organic electrochemical device for noninvasive cortisol sensing *Sci. Adv.* **4** eaar2904
[122] Wang C *et al* 2018 Monitoring of the central blood pressure waveform via a conformal ultrasonic device *Nat. Biomed. Eng.* **2** 687–95
[123] Zhou H, Zhang Y, Qiu Y, Wu H, Qin W, Liao Y, Yu Q and Cheng H 2020 Stretchable piezoelectric energy harvesters and self-powered sensors for wearable and implantable devices *Biosens. Bioelectron.* **168** 112569
[124] Hu X, Ding Z, Fei L and Xiang Y 2019 Wearable piezoelectric nanogenerators based on reduced graphene oxide and *in situ* polarization-enhanced PVDF-TrFE films *J. Mater. Sci.* **54** 6401–9
[125] Wu Y, Qu J, Daoud W A, Wang L and Qi T 2019 Flexible composite-nanofiber based piezo-triboelectric nanogenerators for wearable electronics *J. Mater. Chem.* A **7** 13347–55
[126] Kumar A, Kumar R and Satapathy D K 2020 Bi_2Se_3-PVDF composite: a flexible thermoelectric system *Physica* B **593** 412275
[127] Wang M, Xu Z, Hou Y, Li P, Sun H and Niu Q J 2020 Fabrication of a superhydrophilic PVDF membrane with excellent chemical and mechanical stability for highly efficient emulsion separation *Sep. Purif. Technol.* **251** 117408
[128] Khare D, Basu B and Dubey A K 2020 Electrical stimulation and piezoelectric biomaterials for bone tissue engineering applications *Biomaterials* **258** 120280
[129] Shuai C, Liu G, Yang Y, Yang W, He C, Wang G, Liu Z, Qi F and Peng S 2020 Functionalized $BaTiO_3$ enhances piezoelectric effect towards cell response of bone scaffold *Colloids Surf.* B **185** 110587
[130] Polley C, Distler T, Detsch R, Lund H, Springer A, Boccaccini A R and Seitz H 2020 3D printing of piezoelectric barium titanate-hydroxyapatite scaffolds with interconnected porosity for bone tissue engineering *Materials* **13** 1773
[131] Tariverdian T, Behnamghader A, Milan P B, Barzegar-Bafrooei H and Mozafari M 2019 3D-printed barium strontium titanate-based piezoelectric scaffolds for bone tissue engineering *Ceramics Int.* **45** 14029–38